

Surface structure of cadmium selenide nanocrystallites

A. C. Carter

Naval Research Laboratory, Washington, D.C. 20357

C. E. Bouldin

National Institute of Standards and Technology, Gaithersburg, Maryland 20818

K. M. Kemner and M. I. Bell

Naval Research Laboratory, Washington, D.C. 20357

J. C. Woicik

National Institute of Standards and Technology, Gaithersburg, Maryland 20818

S. A. Majetich

Carnegie Mellon University, Pittsburgh, Pennsylvania 15213

(Received 8 April 1996)

Extended x-ray-absorption fine structure (EXAFS), Fourier-transform infrared absorption (FTIR), and elemental analysis were used on a variety of CdSe nanocrystallites (NC's) to study surface structure. All CdSe NC's were grown by standard inverse micelle techniques. Two sets of NC's samples were made. One set was made so that only the size of the NC's was varied, while the surface treatment was kept the same. The other set was made so that only the surface treatment was varied, while the size distribution was kept the same. For the EXAFS experiments, reference compounds similar in structure were measured. FTIR found surface Cd atoms to be passivated by pyridines and water groups. Fourier-filtered first-shell Cd EXAFS also supports the existence of water groups attached to the surface Cd atoms. The lack of any SeO and Si(CH₃)₃ in the FTIR signal indicates that most surface Se atoms have unterminated bonds. Fourier-filtered first-shell Se EXAFS spectra indicate that Se has only Cd as its first-nearest neighbor, and that the coordination number is reduced from the bulk value, suggesting surface Se atoms are unpassivated. Our data support the existence of surface Se lone-pair orbitals that can trap an optically excited hole. [S0163-1829(97)00908-9]

Nanocrystallites (NC's) represent a domain of condensed matter that is not well understood. The evolution of physical properties with NC size is particularly interesting since very small NC's behave more like molecules, and larger nanocrystallites behave more like bulk material. In addition, NC's have a very large surface to volume ratio, resulting in a system in which surface properties can easily be studied, since typically 10–50 % of the atoms are at the surface.

CdSe NC's are of particular interest because of their potential use as nonlinear optical materials^{1,2} as well as their photochemical properties.^{3–5} Their use in optical devices arises primarily from their concentrated oscillator strength, tunable band gap as a function of NC size,^{6–8} and relaxation properties that depend on surface treatment.^{9–11} In the CdSe nanocrystallites studied here the surface is believed to play a large role in the relaxation properties of optically excited electron-hole (e^-h^+) pairs. A likely relaxation pathway is through a trapped hole state at the surface of the nanocrystallites, where an optically excited hole is trapped at a surface Se atom lone-pair orbital during relaxation.¹² In order for there to be a lone-pair orbital the Se atoms at the surface must be unpassivated.

The applications of CdSe NC's in electrooptic systems depend on understanding the charge transfer mechanism of optically generated carriers out of the NC. This depends critically on the surface structure of the NC's; consequently

the aim of this paper is to determine the surface structure of the CdSe NC's. TEM measurements sometimes observe faceted surfaces on the NC's,¹³ but beyond that, the surfaces appear to be disordered. Therefore, in this work we used extended x-ray-absorption fine structure (EXAFS), Fourier-transform infrared spectroscopy (FTIR), and elemental analysis, which are structural and chemical probes that are useful even in disordered matter.

All of the CdSe NC's samples were made by standard inverse micelle (IM) techniques. The preparation methods are described in detail elsewhere¹⁴ so the synthesis method will only be summarized: The entire synthesis was performed under inert atmosphere and with vigorous stirring. 33.3 g of AOT, dioctyl sulfo succinate, (sigma) was dissolved in 1300 mL *n*-heptane (sigma, capillary GC). 4.3 mL of deionized and degassed water was added and stirred until the microemulsion became homogeneous, after which 1.12 mL of 1 M cadmium perchlorate in water was added and stirred for 2 h. At this point, the molar ratio of water to AOT was 4 (defined $W=[H_2O]/[AOT]$). This ratio determines the average size of the NC's synthesized. W can easily be altered by changing the amount of deionized water added while keeping all other reagents the same, thus a size selected series of NC's can be made. Then 210 μ L (0.93 mmol) of bis(trimethylsilyl)selenide¹⁵ was added to 10 mL *n*-heptane, which was then added all at once to the microemulsion. The

molar ratio of Cd:Se was 1.2, resulting in NC growth that is Se limited. Within seconds the solution began to change color from clear to yellow, orange or red as the NC's grew. When the solution had finished changing color, usually after 5 min, it was assumed that the NC growth had stopped and the surface capping procedure was then performed.

The NC's were capped with pyridine by adding 1 mL of pyridine to the solution, this caused the NC's to precipitate. Surface capping is important because the surface ligands sterically prevent the NC's from touching each other and permanently fusing together. After the surface had been capped with pyridine, the NC's were no longer kept under inert atmosphere. The solution was then centrifuged and the clear supernatant was poured off, leaving only the NC's. The NC's were then redissolved in 15 mL of pyridine with the aid of sonication and then filtered through a 15 μm frit to remove all particulate contaminants and permanently flocculated NC's. 20 mL of hexanes were added to precipitate the NC's, which were then centrifuged, and once again the clear supernatant was poured off. The NC's were dissolved, precipitated, and centrifuged two more times to ensure the high purity required for accurate FTIR and elemental analysis results.

One set of samples was made to give a size-selected series by changing the W of the initial IM solution. Most of the results discussed are from this size-selected group of samples.

A second large batch of NC's were made, at a single size of 35 \AA and then divided into four separate samples for different surface treatment. This division was made to ensure that each sample of NC's had the same size distribution and that only the surface treatment varied. One sample was left untreated as pyridine capped NC's, the other three were redissolved in 15 mL of pyridine and separately capped with hexanethiol, phenylthiol, and 2-naphthalenethiol (Aldrich). For the thiolate capped samples, to ensure that the capping reaction was complete, the amount of thiol compound added was equal to the estimated amount of Cd in the NC samples. The NC's then remained in solution with the thiols for two days to allow a complete reaction.³ The NC's were then washed three times with the above procedure to remove any excess thiol and byproducts of the capping reaction. Absorption spectra were measured to make sure the size distribution of the NC's did not change. After the samples were washed they were allowed to dry in air. Nanocrystallites capped with pyridine, hexanethiolate, phenylthiolate, and 2-naphthalenethiolate will be called Pyr NC's, BuS⁻ NC's, PhS⁻ NC's, and NaphS⁻ NC's, respectively, for the remainder of the text.

The NC's are fabricated in solution, so it is reasonable to expect a mixture of pyridine and water coordinating the surface atoms. With this in mind, $\text{Cd}(\text{ClO}_4)_2 \times x \text{H}_2\text{O} \times y$ pyridine was measured as an EXAFS reference compound, where x and y denote unknown quantities of water and pyridine. It was made by adding $\text{Cd}(\text{ClO}_4)_2 \times 6\text{H}_2\text{O}$ to pyridine and sonicating until no more could dissolve. After centrifugation of the saturated solution the supernatant was decanted and allowed to evaporate under a flow of argon. A crystalline powder very similar to the original $\text{Cd}(\text{ClO}_4)_2 \times 6\text{H}_2\text{O}$ was recovered. FTIR of this substance looked exactly like a linear combination of the FTIR spectra of $\text{Cd}(\text{ClO}_4)_2 \times 6\text{H}_2\text{O}$

and pyridine coordinating to Cd.¹⁶ To establish a quantitative estimate of the $x:y$ ratio we normalized the water and pyridine peaks in the NC FTIR spectra using an elemental analysis (see below, Table II). This normalization approximately accounts for the difference in oscillator strengths between the pyridine and water peaks in the FTIR, allowing peak areas to be used to make a rough estimate of relative abundances. For the $\text{Cd}(\text{ClO}_4)_2 \times x \text{H}_2\text{O} \times y$ pyridine this gives an estimate of $x:y = 1$, to within a factor of two.

Optical absorption spectra were taken on a Hitachi U-3000 Spectrophotometer in a solution by dissolving less than 1 mg of NC powder in 2 mL of pyridine. Powder x-ray diffraction was measured on a Rigaku x-ray diffractometer with a copper rotating anode target on pressed powdered samples. FTIR was performed on a Nicolet 5DXB by grinding 5 mg of the NC powder with 20 mg of KBr and pressing a pellet. Elemental analysis was performed by Galbraith Labs in Tennessee. EXAFS measurements were performed at room and liquid nitrogen temperatures at the X23A2 beamline of the National Synchrotron Light Source at the Brookhaven National Laboratory. The beamline uses Si (311) crystals, which reject the second harmonic of the x-ray beam. Therefore, at the Se K edge of 12 658 eV, the third harmonic passed by the monochromator is at 38 000 eV, and can be neglected. Harmonics are even less important when measuring the Cd K edge at 26 711 eV. The samples were easily crushed into a fine powder and spread thinly and evenly onto the sticky side of scotch transparent tape. To achieve an optimal absorption of about 0.5–1.0 absorption lengths at the Se and Cd edge, the tape had to be layered 36 and 72 times, respectively. All samples were simultaneously measured in transmission and fluorescence mode, but only the transmission data were analyzed because of its better signal-to-noise ratio. EXAFS transmission measurements on bulk CdSe, SeO_2 , $\text{Cd}(\text{ClO}_4)_2 \times 6\text{H}_2\text{O}$, $\text{Cd}(\text{ClO}_4)_2 \times x \text{H}_2\text{O} \times y$ pyridine, and CdCl_2 were used as standards for the EXAFS analysis. All reference materials were fabricated under similar conditions, and measured under the same experimental conditions as the NC's. Under these conditions, transferability of the EXAFS phase and amplitudes is very good, yielding accurate structural results.

Cadmium selenide NC's made by the IM technique are well characterized by TEM and x-ray data in the literature.^{14,17} For this reason only visible optical absorption and powder x-ray diffraction were used for preliminary verification and characterization of the NC samples. Optical absorption spectra were used to estimate the size of the NC's and revealed the broad size distribution that is characteristic of NC's synthesized with the IM technique (Fig. 1). From the optical absorption spectra and the extensive literature on CdSe NC's the size-selected NC's were estimated to be 17 \AA , 20 \AA , 22 \AA , 23 \AA , and 35 \AA with a 10% size distribution. Powder x-ray diffraction on these samples were typical of these kinds of NC's (Fig. 2). The broadening of the x-ray diffraction peaks is primarily due to the reduced coherent scattering length of the NC's.¹⁷

Figure 3 shows the $\chi(k) \cdot k$ data measured at 80 K for the Se and Cd edges of 35 \AA CdSe Pyr NC's. The data are of excellent quality and cover a large range in k space. Data of all the NC's and standards were of similar quality. The analysis proceeded by standard methods:¹⁸ edge-step normal-

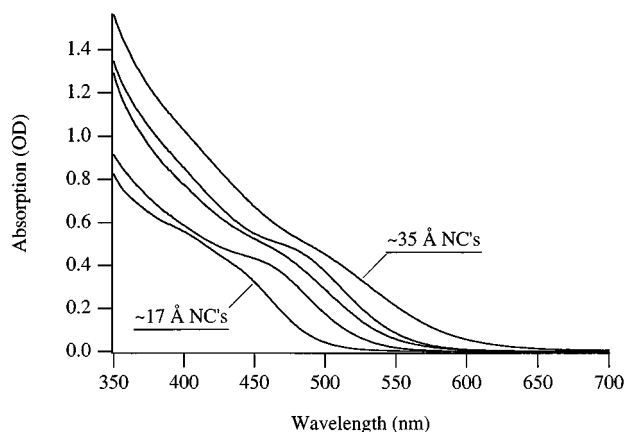


FIG. 1. Optical absorption spectra of CdSe nanocrystallites ranging from 17 to 35 Å in size.

ization, spline background removal, Fourier filtering, and ratio or curve-fitting analysis of first-shell data. Correlation errors in the fitting process were determined by varying parameters to double the residual error relative to the best fit. Variations in the raw experimental data and variations due to slightly different analysis methods were much smaller than correlation errors and not included in the quoted error bar values. Error bars were calculated using only regions of data where the standard reference sample had an influence on the data. For example, even though the Cd EXAFS data for the NC's extended to 15 \AA^{-1} , only data up to 6.35 \AA^{-1} was used for the error determination of the O backscatterer because its contribution to the NC data ceased above that point.

Analysis of the second and higher shells was not attempted, due to their small amplitude. In any case, analysis of the second shell would be complicated by the fact that the NC's are expected to contain at least one stacking fault.¹⁹ One stacking fault will make the two neighboring planes of atoms on each side appear as zinc blende if the NC is mostly wurtzite, or vice versa. There is no difference in the zinc

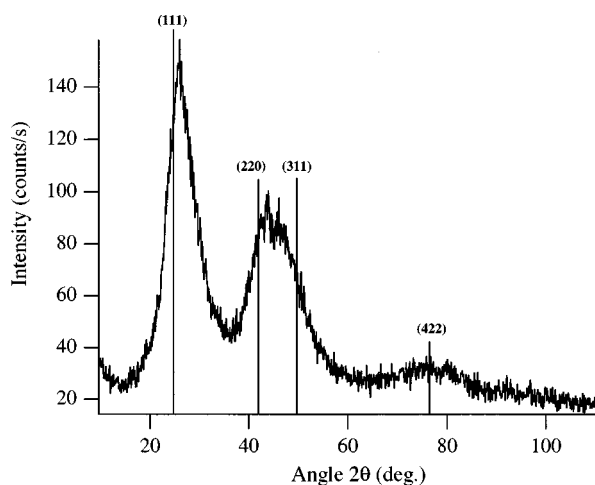


FIG. 2. X-ray powder diffraction of 35 Å CdSe nanocrystallites. Positions of some CdSe bulk zinc-blende peaks are marked. The absence of the CdSe wurtzite peak at $2\theta = 35.1^\circ$ indicates that the NC's are better described as being in the zinc-blende structure.

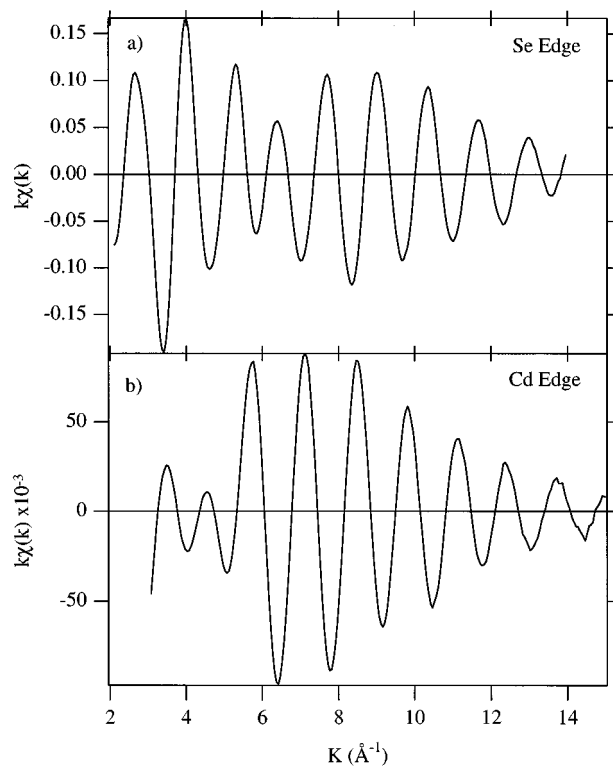


FIG. 3. Typical EXAFS $\chi(k)*k$ of CdSe nanocrystallites. (a) The Se K absorption edge data of a 22 Å nanocrystallite, and (b) the Cd K absorption edge data of a 17 Å nanocrystallite.

blende and wurtzite structures in the first shell, but the change to wurtzite from zinc blende moves one atom from the third shell into the range of the zinc-blende second shell, complicating the analysis of second and higher coordination shells.

Figure 4 shows the Fourier transforms of the $\chi(k)$ data of the bulk CdSe, and all 5 of the CdSe size-selected Pyr NC samples. The reduction of Fourier-transform first-shell peak height for both Cd and Se NC data relative to bulk CdSe indicates a drop in coordination number due to surface truncation. The complete absence of higher order peaks is due to structural disorder in the NC. The small increase in width of the first shell from the bulk to the NC samples indicates only a small bond length disorder, so the absence of higher order peaks is attributed to bond angle disorder, as has been seen before.²⁰ Such disorder is expected in zinc-blende materials that are synthesized at such low temperatures. Amorphous or partially crystallized diamond and zinc-blende materials have been measured many times with EXAFS, and it is always found that the second-shell Debye-Waller factor, which can increase through bond bending, is much larger than in the corresponding bulk crystal.²¹ In contrast, the first-shell Debye-Waller factor can only increase through energetically expensive bond stretching, and remains very close to the bulk value, as we find for the CdSe NC's.

Back transforming the data with a Hanning tapered band pass filter around the first shell revealed much about the NC surfaces. The back transformed data was fit with the empirical standards by adjusting the first-shell distance, coordination number, and Debye-Waller factor to produce a best fit. Almost identical structural parameters were obtained using

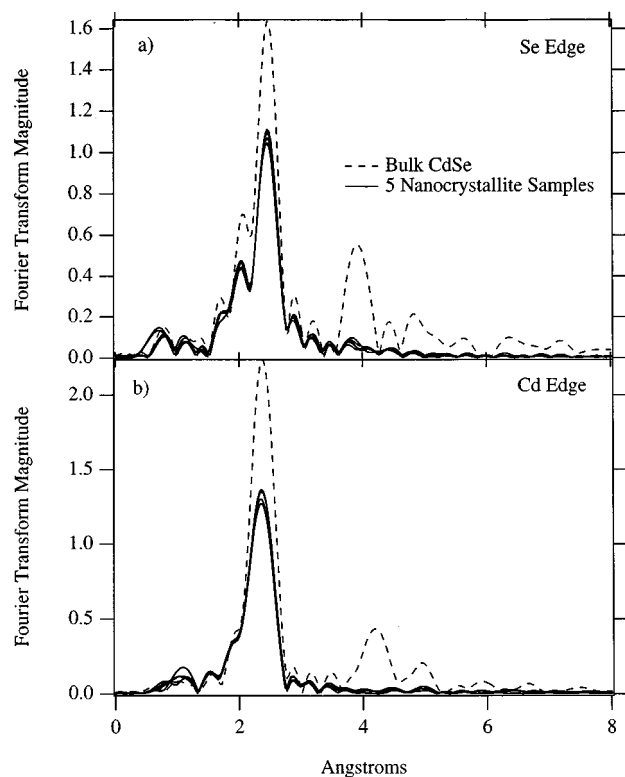


FIG. 4. Fourier transforms of the $\chi(k)$ data for the NC's and bulk CdSe. The dashed line is the bulk CdSe data, and the nanocrystallite data are overplotted as solid lines. The Se-edge data were weighted by k^1 before transforming, and the Cd-edge data were weighted by k^2 . (a) The Se K absorption edge data, and (b) the Cd K absorption edge data. For both edges, the reduction in first-shell peak height is primarily due to increased disorder in the NC's.

the ratio method. The Se-edge data was fit very well even at low k with only bulk CdSe as the Se-Cd standard [Fig. 5(a)]; including additional backscattering atoms always resulted in a poorer fit. Low Z atoms contribute most strongly at low k , but even at low k our Se-edge NC data were accurately fit with only Cd backscatters. From the magnitude of the backscattering amplitude of the oxygen in the SeO_2 empirical reference sample, any significant amount of oxygen bonded to the surface Se atoms would have been observable. The overall reduction in the number of Cd nearest neighbors and the absence of any low Z nearest neighbors suggests that the surface Se atoms are not passivated. This is important because one of the possible relaxation pathways requires the optically excited hole to become trapped by a lone electron pair orbital associated with a surface Se atom that is not passivated. Another study has found evidence of selenium oxygen bonds on their CdSe NC samples, but those NC's were synthesized by a very different technique and CdSe NC's are very synthesis dependent.¹¹ Fitting the Cd-edge first-shell back transform with only bulk CdSe resulted in a poor fit at low k [Fig. 5(b)]. The addition of bulk $\text{Cd}(\text{ClO}_4)_2 \times 6\text{H}_2\text{O}$ to the EXAFS fitting parameters resulted in a very good fit at both high and low k . The Cd atom in $\text{Cd}(\text{ClO}_4)_2 \times 6\text{H}_2\text{O}$ is octahedrally coordinated by 6 H_2O molecules and the ClO_4 groups are then attached to the water molecules. Other first-shell backscattering combinations were tried, including a theoretical (FEFF3) Cd-O

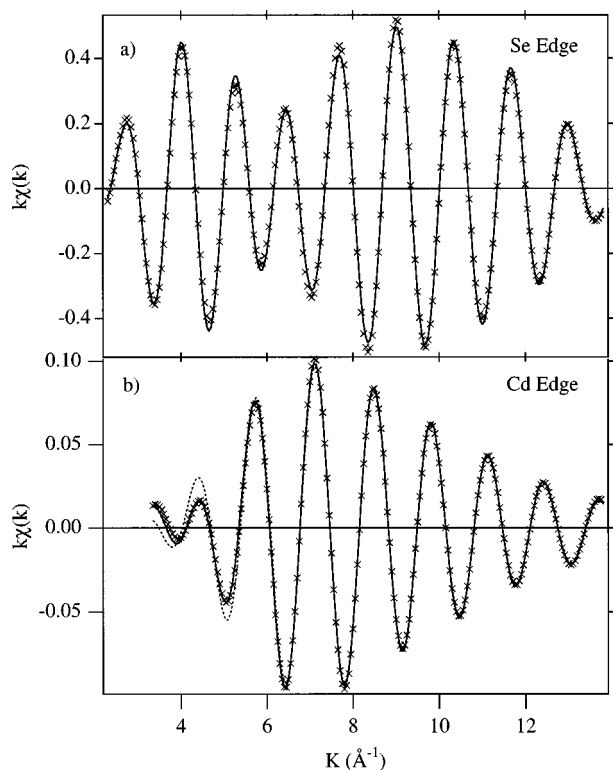


FIG. 5. Fits to the single-shell filtered data of the $\chi(k)*k$ of CdSe nanocrystallites. (a) Se-edge data (x markers), filtered over the range 1.5–3.5 Å in r space, fitted (solid line) with EXAFS data from bulk CdSe. (b) Cd-edge data (x markers) fitted with only bulk CdSe (dashed line) and with both bulk CdSe and $\text{Cd}(\text{ClO}_4)_2 \times 6\text{H}_2\text{O}$ (solid line). The NC data and the bulk CdSe were filtered over an identical range in r space, from 1.32 to 3.01 Å, and the $\text{Cd}(\text{ClO}_4)_2 \times 6\text{H}_2\text{O}$ data were filtered over the range 0.71–2.36-Å.

backscatterer²² and an empirical Cd-Cl backscatterer derived from the CdCl_2 , with poor results. This leads to the conclusion that Cd atoms have both Se and O, in the form of H_2O , as their first-nearest neighbors.

The same fitting process described above was applied to all the CdSe NC samples; the results are summarized in Table I. Within the errors of the analysis the best fit parameters do not change with NC size. This at first seems unexpected because NC's of different size have a different surface to volume ratio and should show a varying first-shell coordination number as a function of NC size (Fig. 6). However, the results of the calculation depicted in Fig. 6 shows that the variation in coordination number from the smallest (17 Å) to the largest (35 Å) NC is only 0.25, well within the error of the EXAFS measurements. We find a coordination number reduction in the NC's relative to the bulk for all the NC samples, and coordination numbers for each NC that are consistent with the model calculation. A significant reduction in coordination number due to internal voids is ruled out by TEM. The data suggest that these samples have an asymmetric size distribution towards smaller NC's because we always find a coordination number that is slightly lower than the model calculation. In addition, we find that the Se coordination around Cd atoms is always slightly lower than the Cd coordination around Se atoms, suggesting that the NC's may

TABLE I. EXAFS structural parameters of CdSe nanocrystallites, measured at 80 K. Error bars are constant across rows in the table. Error bar values are in parenthesis and denote a \pm variation in the final digits of the measured value. Bulk values are listed for reference.

Se <i>K</i> edge results						
Subscript 1 denotes first-shell Cd atoms						
Size	17 Å	20 Å	22 Å	23 Å	35 Å	Bulk
N_1	3.24(35)	3.44	3.40	3.39	3.30	4.000
R_1	2.61(1)	2.615	2.616	2.617	2.618	2.630
$\Delta\sigma_1^2$	0.001 49(10)	0.001 62	0.001 54	0.001 55	0.001 47	0.000 00
Cd <i>K</i> edge results						
Subscript 1 denotes first-shell Se atoms						
Subscript 2 denotes first-shell O atoms						
Size	17 Å	20 Å	22 Å	23 Å	35 Å	Bulk
N_1	3.060(35)	3.16	3.23	3.11	3.12	4.00
R_1	2.62(1)	2.616	2.616	2.618	2.622	2.630
$\Delta\sigma_1^2$	0.001 64(56)	0.001 71	0.001 56	0.001 33	0.001 39	0.000 00
N_2	0.81(31)	0.73	0.86	0.68	0.65	6.00
R_2	2.35(2)	2.344	2.336	2.326	2.337	2.290
$\Delta\sigma_2^2$	0.004 48(43)	0.003 29	0.008 21	0.005 13	0.001 90	0.000 00

be slightly Cd rich at the surface. We also find that the sum of the coordination numbers of the Se and O around the Cd atoms is approximately to 3.9, suggesting that nearly all of the surface Cd atoms have an H_2O group attached. The most notable conclusion from the fitting is that Se atoms have a total coordination of only 3.2–3.4 atoms, compared to the total coordination of ~ 4 around the Cd atoms. This strongly suggests that the Se atoms at the surface of the NC's remain unpassivated.

In addition to fitting with standard reference compounds, the bulk CdSe and all NC samples were measured at 300 and 80 K. The change in temperature alters the amount of thermal broadening, σ , around the first-shell bond length R_1 , and this is usually expressed in terms of $\Delta\sigma^2$ since that reduces

that amplitude of the EXAFS by that factor relative to standard compound, such as bulk CdSe. For all the NC's, irrespective of size, we find $\Delta\sigma^2 = 0.000 40 \text{ \AA}^2$ less than bulk CdSe. These results are about $\Delta\sigma^2 = 0.000 20$ lower than those found by Marcus *et al.*²³ The second-shell of the bulk CdSe reference sample was clearly visible at 80 K and almost completely absent at room temperature, indicating a relatively large thermal component in the bulk second-shell Debye-Waller factor. As has been observed before, for zinc-blende materials, the first-shell Debye Waller factor is reduced by the stiffness of the bond lengths compared to the relatively low energy required to induce bond bending.²¹ The absence of an observable second shell, even at 80 K, in the NC samples indicates that there is a significant static disorder in the tetrahedral bond angle in the interior of the NC's as well as at the surface.

FTIR measurements of the NC's and reference compounds confirm the EXAFS data and provide extra information about the NC surface structure. In the NC spectra there were no Se-O absorption peaks around 890 cm^{-1} as seen in cleaved bulk CdSe that had been oxidized²⁴ (Fig. 7). No bulk SeO_2 absorption peaks were seen in NC spectra either. There is also no sign of $\text{Si}(\text{CH}_3)_3$ groups that would come from the Se starting reagent. These points all support the conclusion of unpassivated surface Se atoms indicated by EXAFS. All IR absorption peaks corresponding to $\text{Cd}(\text{ClO}_4)_2 \times 6\text{H}_2\text{O}$ appear in the NC samples. In conjunction with the EXAFS results, this means that surface Cd atoms first have water bound to them, then ClO_4 groups bound to the water molecules, as in the bulk $\text{Cd}(\text{ClO}_4)_2 \times 6\text{H}_2\text{O}$. In addition, the NC FTIR spectra show strong peaks consistent with pyridine coordinating with Cd atoms as seen in the $\text{Cd}(\text{ClO}_4)_2 \times x \text{H}_2\text{O} \times y$ pyridine standard and reference tables of pyridine coordinating with Cd^{2+} in the form of CdCl_2 .¹⁶ When pyridine is in this state, an absorption peak that normally appears at 603 cm^{-1} shifts to overlap with a very strong

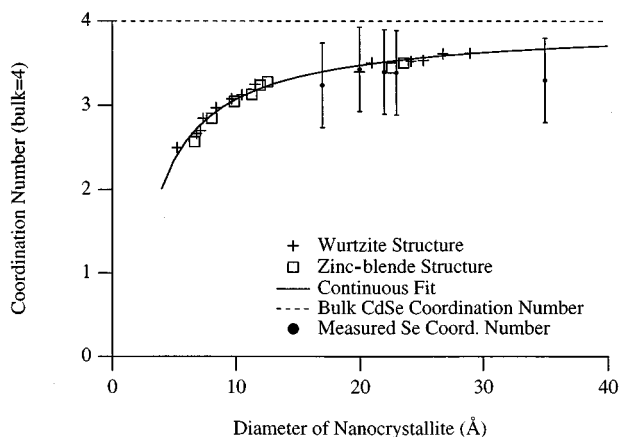


FIG. 6. Model calculation of coordination number versus nanocrystallite size for Wurtzite and Zinc blende structures constructed from a ball-and-stick model. The solid line is a smooth fit to the constructed values at the various discrete sizes. Overplotted, with error bars, are the results of the coordination number determined by Se EXAFS.

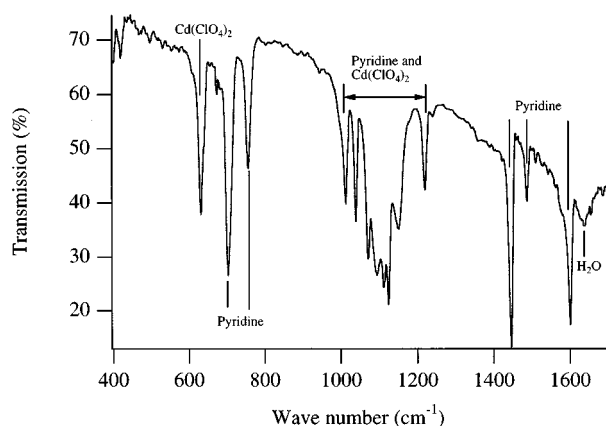


FIG. 7. Fourier-transform infrared spectrum of a typical 35 Å CdSe nanocrystallite sample capped with pyridine. The data show no SeO modes that would be expected to appear at ~ 890 wave numbers, nor any SiCH_3 at ~ 842 wave numbers from the starting reagent, supporting the EXAFS fitting result that the Se surface atoms remain unterminated.

$\text{Cd}(\text{ClO}_4)_2 \times 6\text{H}_2\text{O}$ mode at 626 cm^{-1} . The complete absence of any peak at 603 cm^{-1} means that all pyridine in the sample is bound to Cd. The peak at 1632 cm^{-1} is consistent with an H_2O vibrational mode that is broadened due to dative bonding, as would be the case when a water group is attached to a Cd atom.²⁵

Elemental analysis (Table II) supports the EXAFS and FTIR data and reveals more information about the surfaces of the NC's. The abundance of Cd and Se are approximately the same, suggesting once again that both Se and Cd are at the NC surface. Using a model developed by Alivisatos *et al.*, NC's within the range of 25–35 Å in diameter are approximately 45% surface atoms.¹¹ From the elemental analysis 12% of the total number of atoms are Cd, implying that 5.4% of all atoms are Cd atoms on the surface of the NC. Comparing this to the 5.85% abundance of N implies that there are on average 1.1 pyridines ($\text{C}_5\text{H}_5\text{N}$) attached to each surface Cd atom. Elemental analysis supports the existence of ClO_4 from the detection of Cl. The lack of any silicon suggests the loss of the $\text{Si}(\text{CH}_3)_3$ groups from the Se starting reagent, also in support of bare surface Se atoms. The elemental data is completely consistent with the EXAFS and FTIR.

EXAFS of the $\text{Cd}(\text{ClO}_4)_2 \times x \text{H}_2\text{O} \times y$ pyridine reference compound differed from $\text{CdClO}_4 \times 6\text{H}_2\text{O}$ by a 60% reduction in H_2O coordination number, a very small Debye-Waller factor ($\Delta\sigma^2 = 0.00184$), and a very small change in the radial distance ($\Delta R = 0.05 \text{ \AA}$). This is unexpected because elemental analysis and FTIR suggest an abundance of pyridine coordinating to the Cd atoms. The Cd-N bond length is 2.46 \AA ,²⁶ and the Cd-O bond length is about 2.29 \AA .^{27,28} Oxygen and nitrogen have similar backscattering characteristics and EXAFS is very sensitive to changes in bond length, therefore such a large difference in bond length should have been detectable. This suggests that the N contribution to the EXAFS signal is washed out by disorder in the Cd-pyridine bond length but not in the Cd-water bond length. The Cd-pyridine and Cd- H_2O vibrational modes are similar in energy, 186 cm^{-1} (Ref. 29) and 356 cm^{-1} (Ref. 27), respectively, so

TABLE II. Elemental analysis of 35 Å CdSe nanocrystallites. Abundances were normalized to the elements listed. No elemental analysis was done for oxygen. Quoted errors are only statistical; systematic errors are probably $\sim \pm 10\%$ of the mean values.

Element	Atom %	
Cadmium	11.89	0.30
Selenium	12.98	0.33
Carbon	30.83	0.06
Hydrogen	37.43	0.60
Nitrogen	5.85	0.09
Chlorine	0.97	0.01
Silicon	≤ 0.04	

there should be no significant difference in thermal disorder, therefore the disorder must be static. In the bulk $\text{Cd}(\text{ClO}_4)_2 \times x \text{H}_2\text{O} \times y$ pyridine reference sample this can be understood because the pyridine is being forced into a crystal structure that was originally that of $\text{Cd}(\text{ClO}_4)_2 \times 6\text{H}_2\text{O}$. A similar effect was seen in the NC samples, and we believe that the small H_2O molecules are able to accommodate to irregularities in the surface of the NC, while the much larger pyridine molecules are sterically hindered.

The set of samples with the different surface treatment but the same size distribution showed very little difference in the EXAFS data. Elemental analysis on the 35 Å BuS- NC's indicates approximately only 25 sulfur atoms per NC. This size NC has approximately 310 surface atoms so this would not result in a change in the surface significant enough for EXAFS to resolve. Although elemental analysis was not performed on the PhS- and NaphS- NC samples, we believe that these samples are chemically similar to the BuS- NC, accounting for the nearly identical EXAFS. Any change in surface passivation from the different surface treatments of these NC's is within the error bars of the EXAFS measurements.

In conclusion, the main objective of this work was to determine the nature of the local structural environment around the Cd and Se atoms in CdSe NC's and to determine, if possible, any differences in local environment around the surface atoms compared to those in the interior of the NC. We find that the NC's have nearly the same number of Se and Cd atoms at the surface, since the coordination number reduction of the Cd and Se first-neighbor atoms, relative to bulk CdSe, is nearly the same for each central atom. Elemental analysis also indicates approximately equal numbers of Cd and Se atoms, and TEM results lessen the possibility of internal voids, which is the only other mechanism for producing a reduced coordination number.

The Se first neighbors are only Cd atoms. The EXAFS data show no evidence of any oxygen or other low Z atoms in the Se first shell, suggesting that there are unterminated Se bonds at the surface in the form of lone electron pair orbitals. This result supports the theory that optically excited holes can become trapped in long lived ($\sim 100 \text{ ns}$) surface states associated with these orbitals.¹⁶ FTIR measurements also observe no Se-O vibrational modes.

In contrast to the Se environment, the average Cd local environment is clearly a superposition of interior Cd atoms

that are fully coordinated with Se neighbors, and surface Cd atoms that are bonded to Se neighbors as well as to surface passivating ligands. The surface passivation consists of pyridine and H₂O. EXAFS, FTIR, and elemental analysis indicate that H₂O, and pyridine bond to surface Cd atoms, with the ClO₄ bridging to Cd atoms through the H₂O molecules.

Passivation of the surface depends on electrostatic attraction between the surface atoms of the NC and the various passivating ligands. The interior of the NC's is strongly constrained by the geometry of covalent CdSe bonds, but the surface passivation has no such constraints. The electrostatic potential at the surface of the NC must have peaks and valleys similar to the surface of a golf ball. A reasonable picture is that the water molecules of hydrated ClO₄ ions sit in the dimples of the "golf ball." The hydrated ClO₄ ions could terminally bond to one Cd atom or bridge two or three surface Cd atoms while staddling a surface Se atom. The planar pyridine molecules could then orient themselves to fit in next to the hydrating water molecules on the same Cd atoms or bond to other Cd atoms that are not passivated by hydrated ClO₄ ions.

In the first shell around both the Se and Cd atoms we find essentially no change in the first-neighbor distance, a substantial increase in the static disorder, and very little change in the temperature dependence of the Debye-Waller factor. This is the result expected from the nucleation of small particles of a zinc-blende structure at the low temperatures used

in our synthesis. Higher coordination shells are virtually absent, compared with a bulk CdSe standard. There are two reasons: first, in the second shell a much larger proportion of the atoms are sufficiently near the surface of the NC to suffer a substantial coordination number reduction, and, second, the Debye-Waller factor in the second shell is greatly increased relative to the bulk due to bond angle disorder.^{30,31}

The coordination number reduction observed in our samples is close to the reduction that we expect due to missing Cd or Se first-neighbor atoms at the surface of the NC's. From TEM studies, we do not attribute the coordination number reduction to internal voids, but only to the lower coordination number around surface atoms. The low Cd coordination number of the 35 Å NC suggests the presence of very small NC's in the size distribution. We believe that the tails of the size distribution determined from the optical measurements extend considerably beyond the full width at half maximum of 10% for samples made by microemulsion. This would explain why EXAFS finds the first shell coordination to be nearly independent of the particle size determined from optical absorption.

A.C.C. and K.M.K. acknowledge the Naval Research Laboratory/National Research Council for support. The X23A2 beamline is supported by NIST. We would like to thank Dr. Susan Rose-Pehrsson for use of the Hitachi U-3000 Spectrophotometer.

-
- ¹R. K. Jain and R. C. Lind, *J. Opt. Soc. Am.* **73**, 647 (1983).
²E. Hanamura, *Phys. Rev. B* **37**, 1273 (1988).
³S. A. Majetich, A. C. Carter, J. Belot, and R. D. McCullough, *J. Phys. Chem.* **98**, 13 705 (1994).
⁴J. Kuczynski and J. K. Thomas, *Chem. Phys. Lett.* **88**, 445 (1982).
⁵M. J. Natan, J. W. Thackeray, and M. S. Wrighton, *J. Phys. Chem.* **90**, 4089 (1986).
⁶Al. L. Efros and A. L. Efros, *Sov. Phys. Semicond.* **16**, 772 (1982).
⁷L. Brus, *IEEE J. Quantum Electron.* **QE-22**, 1909 (1986).
⁸M. G. Bawendi, M. L. Steigerwald, and L. E. Brus, *Ann. Rev. Phys. Chem.* **40**, 477 (1990).
⁹S. A. Majetich and A. C. Carter, *J. Phys. Chem.* **97**, 8727 (1993).
¹⁰M. Nirmal, C. B. Murray, D. J. Norris, and M. G. Bawendi, *Z. Phys. D* **26**, 361 (1993).
¹¹J. E. Bowen-Katari, V. L. Colvin, and A. P. Alivisatos, *J. Phys. Chem.* **98**, 4109 (1994).
¹²M. G. Bawendi, P. J. Carroll, W. L. Wilson, and L. E. Brus, *J. Chem. Phys.* **96**, 946 (1992).
¹³A. P. Alivisatos, *MRS Bull.* **20**, 23 (1995).
¹⁴M. L. Steigerwald, A. P. Alivisatos, J. M. Gibson, T. D. Harris, R. Kortan, A. J. Muller, A. M. Thayer, T. M. Duncan, D. C. Douglass, and L. E. Brus, *J. Am. Chem. Soc.* **110**, 3046 (1988).
¹⁵M. R. Detty and M. D. Seidler, *J. Org. Chem.* **47**, 1354 (1982).
¹⁶R. J. H. Clark and C. S. Williams, *Inorg. Chem.* **4**, 350 (1965).
¹⁷M. G. Bawendi, A. R. Kortan, M. L. Steigerwald, and L. E. Brus, *J. Chem. Phys.* **91**, 7282 (1989).
¹⁸D. E. Sayers and B. A. Bunker, in *X-ray Absorption: Principles, Applications, Techniques of EXAFS, SEXAFS, and XANES*, edited by D. C. Konigsberger and R. Prins (Wiley, New York, 1988), Chap. 6.
¹⁹C. B. Murray, D. J. Norris, and M. G. Bawendi, *J. Am. Chem. Soc.* **115**, 8706 (1993).
²⁰M. A. Marcus, L. E. Brus, C. Murray, M. G. Bawendi, A. Prasad, and A. P. Alivisatos, *Nano. Mater.* **1**, 323 (1992).
²¹E. A. Stern, C. E. Bouldin, B. Von Rodern, and J. Azoulay, *Phys. Rev. B* **27**, 6557 (1983).
²²J. Mustre de Leon, J. J. Rehr, S. I. Zabinsky, and R. C. Albers, *Phys. Rev. B* **44**, 4146 (1991).
²³M. A. Marcus, W. Flood, M. Steigerwald, L. Brus, and M. Bawendi, *J. Phys. Chem.* **95**, 1372 (1991).
²⁴K. Matsuo, R. Matsuo, and K. N. Fukuoka, *Univ. Rev. Technol. Sci.* **43**, 291 (1989).
²⁵P. Bergstrom, J. Lindgren, M. Sandstrom, and Y. Zhou, *Inorg. Chem.* **31**, 150 (1992).
²⁶R. Zannetti, *Gazz. Chim. Ital.* **90**, 1428 (1960).
²⁷R. Akesson, L. G. M. Pettersson, M. Sandstrom, and U. Wahlgren, *J. Am. Chem. Soc.* **116**, 8691 (1994).
²⁸R. Caminiti and G. Johansson, *Acta Chem. Scand. A* **35**, 373 (1981).
²⁹S. Suzuki and W. J. Orville-Thomas, *J. Mol. Struct.* **37**, 321 (1977).
³⁰J. C. Woicik, T. Kendelewicz, K. E. Miyano, M. Richter, C. E. Bouldin, P. Pianetta, and W. E. Spicer, *Phys. Rev. B* **46**, 9869 (1992).
³¹*X-Ray Diffraction of Ions in Aqueous Solution: Hydration and Complex Formation*, edited by M. Magini (CRC Press, Boca Raton, FL, 1988).